Please verify that (1) all pages are present, (2) all figures are acceptable, (3) all fonts and special characters are correct, and (4) all text and figures fit within the margin lines shown on this review document. Return to your MySPIE ToDo list and approve or disapprove this submission.

SAND2006-7084C

Mid-Infrared Electroluminescence from InAs Self-Assembled Quantum Dots

D. Wasserman[*a], S.H. Howard[a], C. Gmachl[a], S.A. Lyon[a], J. Cederberg[b], and E.A. Shaner[b]
[a]Department of Electrical Engineering, Princeton University, Princeton, NJ, USA 08544;
[**b]Sandia National Laboratories, P.O. Box 5800, Albuquerque, NM 87185

ABSTRACT

Electroluminescence from self-assembled InAs quantum dots in cascade-like unipolar heterostructures is demonstrated. Initial results show weak luminescence signals in the mid-infrared from such structures, though more recent designs exhibit significantly stronger luminescence with improved designs of the active region of these devices. Further studies of mid-infrared emitting quantum dot structures have shown anisotropically polarized emission at multiple wavelengths. A qualitative explanation of such luminescence is developed and used to understand the growth morphology of buried quantum dots grown on AlAs layers. Finally, a novel design for future mid-infrared quantum dot emitters, intended to increase excited state scattering times and, at the same time, more efficiently extract carriers from the lowest states of our quantum dots, is presented,.

Keywords: Mid-infrared, quantum dots, electroluminescence, polarized emission, growth morphology

1. INTRODUCTION

The mid-infrared (mid-IR) spectral range is of significant interest for numerous applications such as trace gas sensing, explosives detection and optical communication. The development of the quantum cascade laser (QCL) [1] has provided compact and robust mid-infrared light sources of significant power [2] and wavelength flexibility [3] for just such applications. Nonetheless, operational challenges to these exceptional light sources do exist, and the two most commonly cited are short scattering times in the upper states of QCL lasers and the difficulty in obtaining vertical laser emission from such structures. By moving from the one-dimensional confinement for quantum well states in QCLs towards the higher confinement of quantum wires or quantum dots, it believed that these challenges can be overcome, and more efficient mid-IR lasers can be developed [4].

The incorporation of three-dimensional confinement of carriers into a quantum cascade (QC) active region results in a significant increase in non-radiative scattering times from the upper laser state, the so-called 'phonon bottleneck'. This result is due to the quantization of electron energy states in three dimensions, which quenches optical phonon scattering from the upper state, except in the case where this state is separated from a final state by a multiple of the optical phonon energy. Earlier studies in QCLs have demonstrated clear evidence for the phonon bottleneck [4] by studying laser emission as a function of magnetic field. In these studies, quantization is provided by the Landau Levels formed in high magnetic fields, and distinct quenching of laser emission is noted as the Landau level splitting due to the magnetic field coincides with optical phonon resonances. Conversely, enhanced emission is seen from these devices when the Landau Level splitting is far from such resonances, leading to a factor of two decrease in the threshold current density of the laser.

Because QCL emission is a result of optical transitions in quantum wells, this emission must be TM-polarized, resulting in edge-emitting lasers. Transitions within the conduction band of quantum dots, however, are between states confined in the lateral direction, as opposed to the growth direction, so light emission from transitions between such states can be seen normal to the growth surface of the sample. This allows for the possible fabrication of mid-IR vertical-emitting

[*] dw@princeton.edu
[**] Sandia is a multiprogram laboratory operated by Sandia Corporation, a Lockheed Martin Company, for the United States Department of Energy's National Nuclear Security Administration under contract DE-AC04-94AL85000.

SPIE USE: ____ DB Check, ____ Prod Check, Notes:

Please verify that (1) all pages are present, (2) all figures are acceptable, (3) all fonts and special characters are correct, and (4) all text and figures fit within the margin lines shown on this review document. Return to your MySPIE ToDo list and approve or disapprove this submission.

lasers, something which is feasible with QCLs only utilizing processing-intensive fabrication techniques such as photonic crystal cavities [5] or second-order diffraction grating on the laser ridge [6].

Thus, while QCLs are without question the current state-of-the-art semiconductor lasers for mid-IR applications, there exists room for the emergence of new, quantum dot-based emitters making use of the three dimensional confinement provided by these self-assembled nanostructures to develop efficient, surface-emitting devices.

In this paper we discuss recent developments in quantum dot based mid-IR emitters. The first example of mid-IR electroluminescence from unipolar quantum dot devices is demonstrated, and subsequent improvements in device and fabrication are discussed. Additionally, we multiple wavelength mid-IR emission from InAs QDs, and demonstrate how the polarization of the emitted structure allows insight into QD growth morphology. Finally, a proposed method for increased efficiency of mid-IR QD emitters is discussed.

2. SAMPLE GROWTH AND DESIGN

The basic sample design of mid-IR QD emitters is very similar, schematically, to the design of QCLs. The devices are designed to inject electrons into excited quantum dot states and force an optical transition to lower QD states. In order to prevent electrons from tunneling directly through the dot layer, a heterostructure energy filter is grown on the downstream side of the QD layer. This filter is especially designed to prevent electron transport at the injection energy while allowing electron escape from the dots at lower energy levels, the effect of which, ideally, is to depopulate the lower QD states, 'making room' for the next optical transition from an excited QD state.

All of the mid-IR emitters discussed herein were grown in a Varian Gen II Molecular Beam Epitaxy system on (001)-oriented n+ GaAs wafers. Each sample consists of an n-doped (~$1x10^{17}$ cm^{-3}) buffer layer, followed by an injection layer designed to inject carriers into excited quantum dot electron states. The QD layer is grown upon the injection layer. The QD layer consists of 2.3 monolayers (ML) equivalent InAs thickness, and is grown at a lowered substrate temperature (520 ºC). The QD layer is followed by a 30s growth interrupt, after which is grown the electron energy filter. Emitter devices were fabricated using evaporated and annealed concentric ring Pd/Ge contacts on square mesa structures.

The samples were then mounted on a copper heatsink blocks and surface emission was studied at 77K with a Nicolet 8700 Fourier Transform Infrared (FTIR) spectrometer using a lock-in step-scan technique. Samples were driven with pulses from 2 to 10 A/cm^2 at 20 kHz with 20µs pulse widths. Emission saturated at low current densities (5 A/cm^2) and spectral shape did not change as a function of current density for any of the samples discussed.

2.1 Sample A

Sample A was an early design, utilizing a basic tunnel injection barrier consisting of 40 Å of $Al_{0.3}Ga_{0.7}As$ followed by 10 Å of AlAs. Injection into excited QD states, for this device, was achieved utilizing the field dropped across the injection barrier. The electron energy filter for sample A consists of an $Al_{0.35}Ga_{0.65}As$/GaAs (79 Å /17 Å) superlattice, with two allowed electron energy minibands below the $Al_{0.35}Ga_{0.65}As$ bandedge. A schematic of the sample A band structure under applied bias is shown in Figure 1(b).

2.2 Sample B

Sample B improved on the design of sample A by utilizing a graded AlGaAs injector in place of Sample A's AlGaAs/AlAs injection barrier. The graded AlGaAs injection barrier, from GaAs to $Al_{0.2}Ga_{0.8}As$, guarantees injection into QD states well above the GaAs bandedge. The electron energy filter for sample B is also simplified, utilizing a double-barrier quantum well in place of the superlattice filter. The quantum well uses two AlGaAs barriers (23 Å each) surrounding a 51 Å GaAs layer. The quantum well is designed such that the lower state is close to the GaAs bandedge, while the upper state sits above the electron injection energy. A schematic of the sample B band structure under applied bias is shown in Figure 2(b).

2.3 Sample C

Sample C, in effect, is a combination of Samples A and B. Sample C utilizes the graded AlGaAs injector of Sample B, and the superlattice filter of Sample A. A schematic of the Sample C band structure under bias is shown in Figure 3(b).

SPIE USE: ____ DB Check, ____ Prod Check, Notes:

Please verify that (1) all pages are present, (2) all figures are acceptable, (3) all fonts and special characters are correct, and (4) all text and figures fit within the margin lines shown on this review document. Return to your MySPIE ToDo list and approve or disapprove this submission.

3. RESULTS AND DISCUSSION

All three samples showed clear electroluminescence in the mid-IR. Initial concerns that the emitted light could be caused by heating effects were dispelled by noting that not only does emission saturate as a function of current, but for each of the spectra shown, with the possible exception of Sample C, all electroluminescence emission spectral signatures peak and decrease well before the detector cut-off energy, unlike a typical heat signal. Furthermore, Sample A was grown both with and without the InAs layer; only the wafer with InAs showed any sign of luminescence.

3.1 Sample A Results

Sample A showed electroluminescence, at 80K, centered at approximately 140 meV (Figure 1(a)). The weak luminescence of this structure, it is believed, is due to the rather inefficient injection method. The injection energy, relative to the GaAs bandedge, is rather low, as carriers gain only the energy dropped across the 50 Å AlGaAs/AlAs barrier. This suggests that the population of the upper energy states in the QD layer will be small, as the majority of electrons will be injected below these states. Additionally, those electrons which are injected into an upper QD state and transition to the QD ground state will find themselves well below the GaAs bandedge. Thus, not only is injection into upper states weak, but extraction from QD ground states will be slow as well, making for an inefficient device.

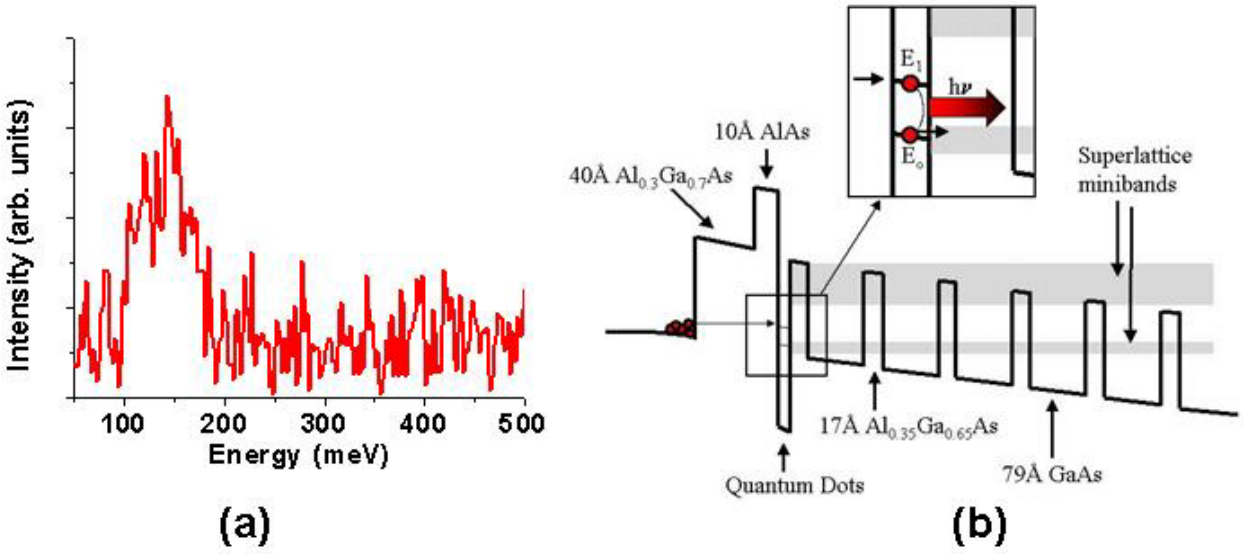

Fig. 1. (a) Electroluminescence spectrum of Sample A at 80K. (b) Conduction band structure schematic for Sample A under applied bias. Electrons are injected from the left, through the 50 Å AlGaAs/AlAs injection barrier, into the InAs quantum dot layer, depicted for clarity as a deep quantum well. Tunneling directly through the QDs is prevented by the miniband structure of the superlattice, which acts as an electron filter. The inset of (b) shows an *idealized* expanded view of the QD active region. In actuality, it is believed that the majority of QD ground states lie well below the GaAs bandedge.

3.2 Sample B Results

Electroluminescence at 80K for Sample B peaked at 130meV (Figure 2(a)), and showed significantly stronger emission than previous samples, as can be seen by the markedly stronger signal to noise ratio of Sample B's spectrum, when compared to Sample A. The increase in electroluminescence intensity is attributed to the improved injector design of this structure (Figure 2(b)). In place of Sample A's AlGaAs/AlAs injection barrier, a graded AlGaAs injector ($Al_xGa_{(1-x)}As$ with x=0 to x=0.2) was used to inject electrons well above the GaAs bandedge. The increase in injection energy increases the population of excitied electron states in the QD layer. The increase in upper state population allows a greater number of intersublevel transitions within the dots, and thus increases mid-

Please verify that (1) all pages are present, (2) all figures are acceptable, (3) all fonts and special characters are correct, and (4) all text and figures fit within the margin lines shown on this review document. Return to your MySPIE ToDo list and approve or disapprove this submission.

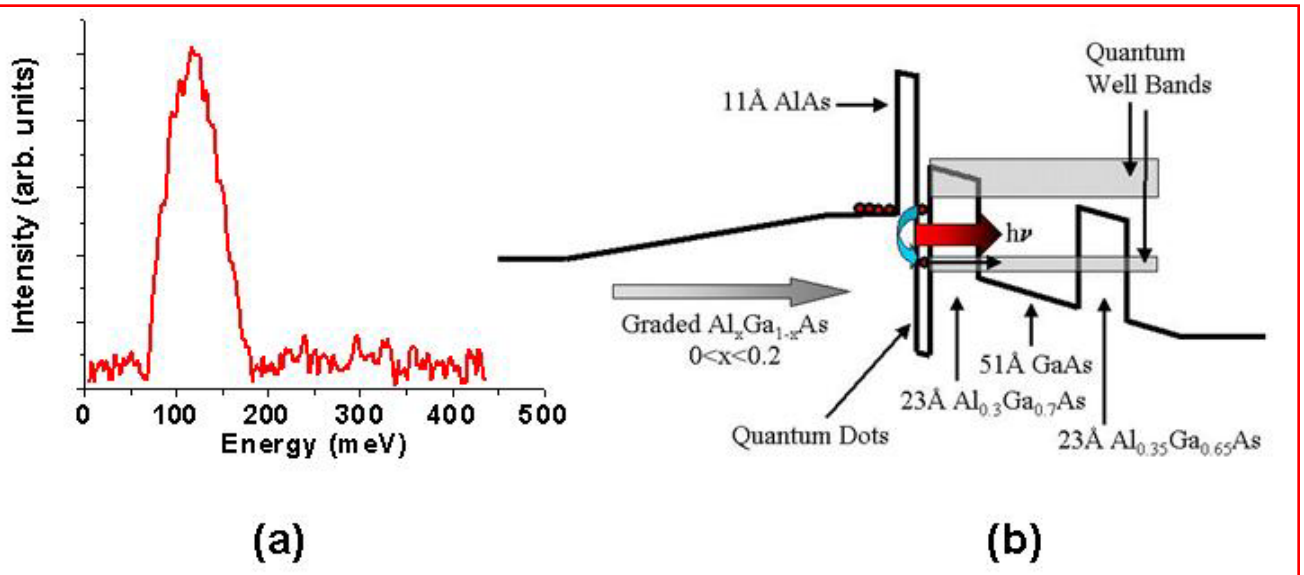

Fig. 2. (a) Electroluminescence spectrum for Sample B at 80K. The marked improvement in emission efficiency from Sample A can be seen by the dramatic increase in signal to noise for the Sample B spectrum. (b) Conduction band structure for Sample B. Electrons are injected from the left side of the structure via a graded AlGaAs injector, which ensures injection into the upper QD states. The quantum dots in this schematic are depicted as a deep quantum well. The electron energy filter for Sample B is achieved by using the states of a AlGaAs/GaAs quantum well.

IR emission from the QD layer. A quantum well electron energy filter is used for Sample B in place of Sample A's superlattice filter. The quantum well filter used is designed such that the lower quantum well state sits near the GaAs bandedge, to allow efficient escape from lower QD states. Photoluminescence measurements of this structure, however, suggest that the majority of QD ground states are still below the GaAs bandedge, so escape from the lower states of dots requires either thermal excitation or a tunneling process, which would lower the efficiency of the device.

3.3 Sample C Results

Electroluminescence at 80K for Sample C shows two distinct emission peaks (Figure 3(a)), a lower energy peak at approximately 100meV, and a second, higher energy, broader signal centered at 170meV. Sample C shows similar emission intensity to that of Sample B, and significantly stronger emission than Sample A. The unique spectrum of Sample C suggests a somewhat different emission process than that for Samples A and B. In this case, emission is seen from two distinct transitions within the sample. Because Sample C employs the graded AlGaAs injector of Sample B, the higher electron injection energy allows the probing of higher QD states, when compared to Sample A. The difference in the spectra of Samples B and C, however, cannot be attributed to the injector region, as the two samples share the same injection structure, and instead can be attributed to the difference in the QD layers of each of the two samples, which is most likely a result of the different capping of the dots. Because the QD layer in Sample B is capped with 23 Å of AlGaAs, whereas the immediate cap of the QD layer in Sample C is a thin AlAs layer (11 Å) (Figure 3(b)), the electronic structure of the dots in Sample C could be markedly different then that of dots in Sample B.

SPIE USE: ____ DB Check, ____ Prod Check, Notes:

Please verify that (1) all pages are present, (2) all figures are acceptable, (3) all fonts and special characters are correct, and (4) all text and figures fit within the margin lines shown on this review document. Return to your MySPIE ToDo list and approve or disapprove this submission.

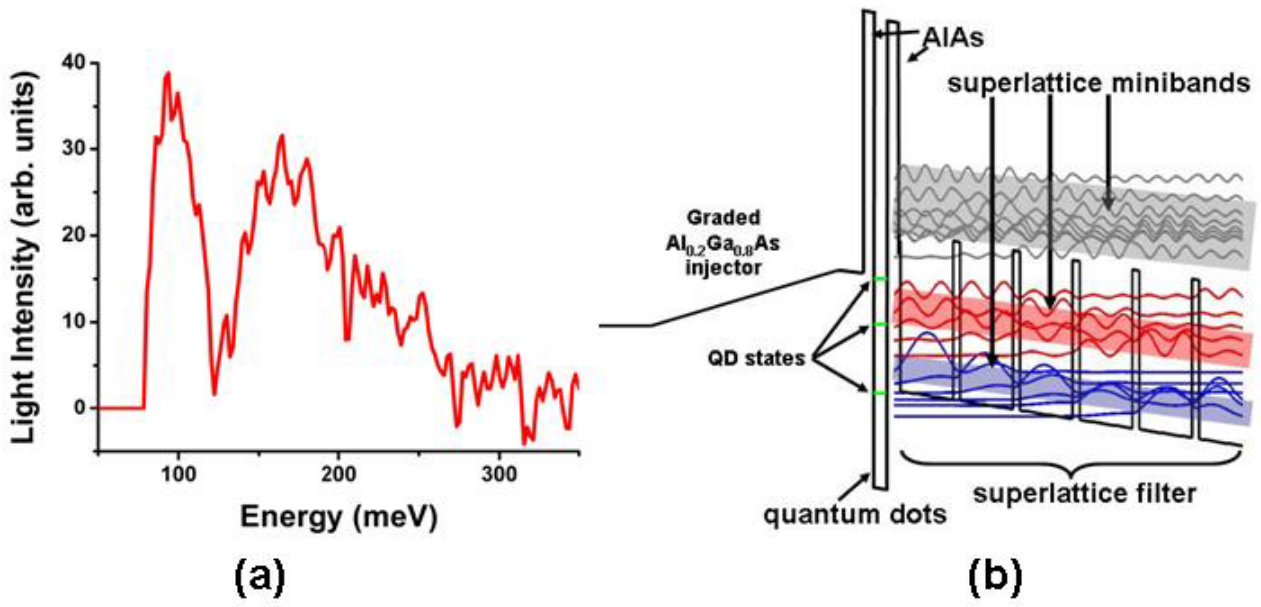

Fig. 3. (a) Electroluminescence spectrum for Sample C at 80K. Sample C emits at two distinct wavelengths, one centered at approximately 100 meV, the other at 170 meV. (b) Conduction band structure for Sample C under bias. As in Sample B, electrons are injected from the left of the structure via a graded AlGaAs injector, though in Sample C, the electron energy filter is provided by the same superlattice used for Sample A. In this figure, the electron wavefunctions making up the energy minibands are depicted, while the shaded region shows the calculated miniband of the structure.

To further study the emission from Sample C, polarization spectroscopy studies were undertaken. In this experiment, the electroluminescence from the QD sample was studied as a function of polarization in the growth plane. A distinct difference was seen in the emission spectra for polarization in the (011) and $(0\bar{1}1)$ crystallographic directions. The spectra for $(0\bar{1}1)$-polarized electroluminescence is shown in Figure 4(a), while that of (011)-polarized emission is shown in Figure 4(b). The emission polarization as a function of energy for these studies was then calculated using the expressions shown in equations 1(a) and 1(b).

$$P_{011}(E) = \left[I_{011}(E) - I_{0\bar{1}1}(E)\right)/\left(I_{011}(E) + I_{0\bar{1}1}(E)\right] \quad (1a)$$

$$P_{0\bar{1}1}(E) = \left[I_{0\bar{1}1}(E) - I_{011}(E)\right)/\left(I_{011}(E) + I_{0\bar{1}1}(E)\right] \quad (1b)$$

Where $I_x(E)$ refers to the emission intensity in the *x* polarization for a given energy. Thus a value of 1 for the polarization indicates a completely polarized signal, while a value of 0 indicates unpolarized emission. The higher energy emission peak, centered at 170 meV was found to be polarized in the (011) direction $(P_{(011)}(170\ meV) \cong 0.41)$, while the lower energy emission peak, center at 100meV, was found to be polarized in the orthogonal $(0\bar{1}1)$ direction $(P_{(0\bar{1}1)}(100\ meV) \cong 0.27)$. The distinct polarization of the two peaks suggests emission from two separate transitions within individual quantum dots.

To better understand this, one can quantitatively model a quantum dot as a "quantum box" with infinite potential barriers and dimensions L_x, L_y, and L_z, where L_x and L_y are the box dimensions in the growth plane and L_z corresponds to the box height in the growth direction. While admittedly a crude approximation, such a model allows for a qualitative understanding of the polarized emission. To more accurately simulate an actual quantum dot, we do not consider quantization in the growth direction, as the tight confinement in this direction pushes the excited states well above the energy range we are considering.

SPIE USE: ____ DB Check, ____ Prod Check, Notes:

Please verify that (1) all pages are present, (2) all figures are acceptable, (3) all fonts and special characters are correct, and (4) all text and figures fit within the margin lines shown on this review document. Return to your MySPIE ToDo list and approve or disapprove this submission.

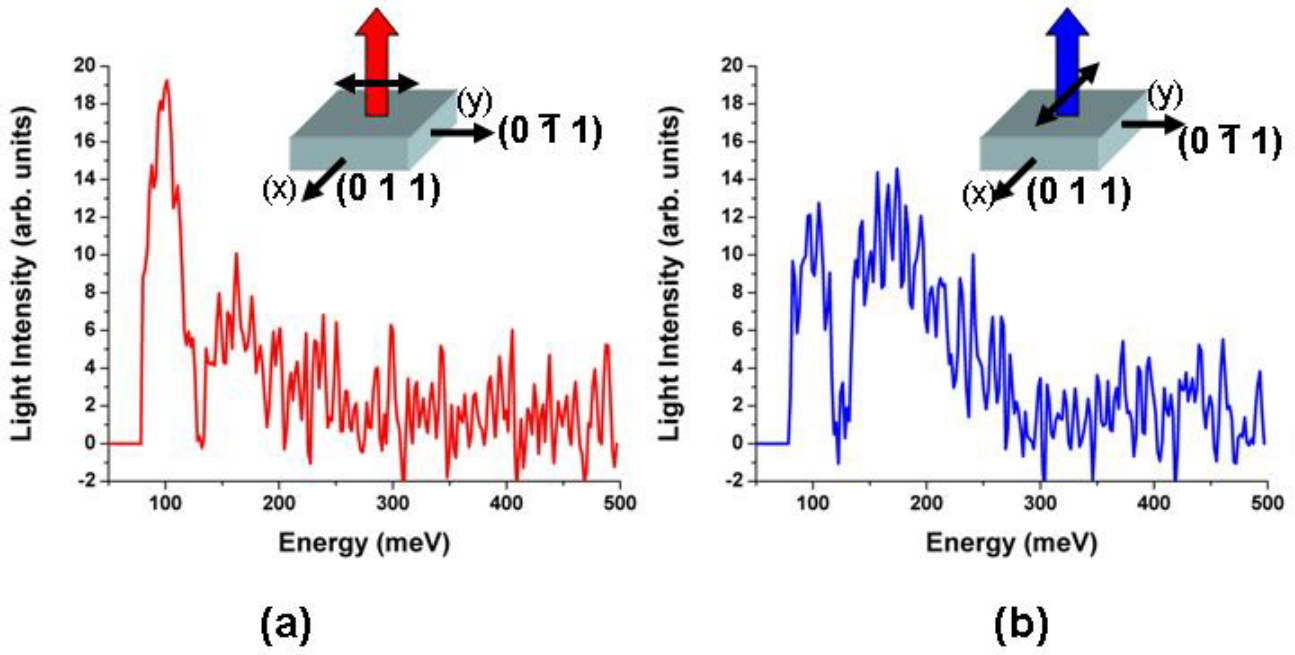

Fig. 4. (a) $(0\bar{1}1)$-polarized electroluminescence from Sample C at 80K. The $(0\bar{1}1)$-polarized spectrum shows significantly stronger luminescence at the lower energy peak, while emission from the higher energy transition is quenched. (b) (011)-polarized electroluminescence from Sample C at 80K. The (011)-polarized spectrum shows significantly stronger luminescence at the higher energy peak, though some luminescence is still seen at lower energies. The weaker polarization of the lower energy peak may be a result of the unpolarized heating signal which is stronger at lower energies.

For a quantum box with sides of equal length ($L_x = L_y$), the first two excited states will be degenerate, and light generated by optical transitions from these excited states to the quantum dot ground state will show no net polarization. If, however, the box is 'stretched', such that $L_x > L_y$, the degeneracy of the excited states is broken, and two distinct emission signal will be seen, a higher energy signal polarized in the y direction, and a lower energy signal polarized in the x direction. The luminescence spectra obtained in our studies, analyzed using the 'quantum box' model, suggest an elongation of our quantum dots in the $(0\bar{1}1)$ direction. Anisotropic quantum dot morphology has been previously observed in *in situ* studies of InAs growth on AlAs surfaces [7]. Additionally, polarization dependent photoconductivity for surface incident mid-IR radiation has also been observed for InAs dots grown on InAlAs lattice-matched to InP [8]. This study also attributed their polarization-dependent spectra to asymmetric QD shape. However, to our knowledge, the data presented here is the first example of polarized light emission in a mid-IR luminescence spectrum from QDs.

The implications of this result are two-fold. First, the observation of dual-wavelength emission broadens the potential spectral range for QD mid-IR emitters, and suggests the possibility of designing mid-IR QD lasers for multiple wavelength emission. Secondly, the study of emission polarization allows for insight into the growth morphology of our InAs QDs using luminescence studies, as opposed to the more common absorption or surface microscopy techniques, the latter of which may not accurately reflect QD morphology, as overgrowth can play a significant role in the final size and shape of these nanostructures.

SPIE USE: ____ DB Check, ____ Prod Check, Notes:

Please verify that (1) all pages are present, (2) all figures are acceptable, (3) all fonts and special characters are correct, and (4) all text and figures fit within the margin lines shown on this review document. Return to your MySPIE ToDo list and approve or disapprove this submission.

3.4 Improvements in Device Design, Growth, and Fabrication

As we move towards the design of QD-based mid-IR lasers, significant improvements in sample design, growth and fabrication will be required. Of concern is the weak emission signal from these devices, which suggests there is ample room for improvement before we begin to see gain in our devices. A closer study of our devices, however, suggests that increasing emission intensity may not as difficult as initially expected. The contacts used for the spectra shown in this paper were large-area grid contacts, patterned on the millimeter length scale (Figure 5(a) inset). Recently, 20 μm pitch grating contacts consisting of 10μm lines with 10 μm spacers (200 μm x 200μm total contact area) were used to contact Sample B (Figure 5(b) inset). While the total area of these contacts was over two orders of magnitude smaller than our typical grid contacts, the total length of contact metal (including grating or grid lines) remained on the same order of magnitude. Luminescence intensity from the grating contact devices was comparable to those samples utilizing large-area grid contacts, suggesting that our large-area grid contacts electrically access only a small fraction of our dots, due to weak current spreading. While the total area of the grating contacts is significantly smaller than the large-area grid contacts, the close spacing of the grid lines allows a higher percentage of the underlying dots to be electrically accessible, leading to comparable emission intensities.

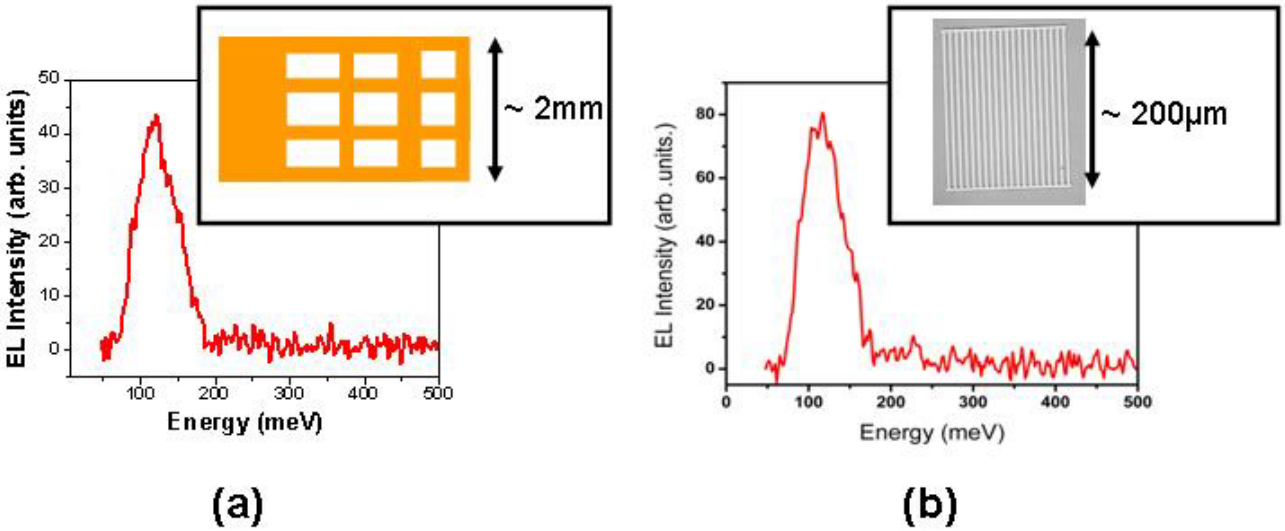

Fig. 5. Comparison of contact geometries used for Sample B. (a) Spectrum from a typical large area contact pad used for electroluminescence studies. The pad geometry consists of a large-area (2mm x 4mm) metal grid with 400 μm grid spacing. (b) Spectrum from a small-area grating contact pad used for electroluminescence studies. The pad geometry consists of a grating with 20μm pitch with 10 μm wide metal lines. Electroluminescence intensity from the grating contact is comparable, if not stronger than that of the large-area pad.

Nonetheless, more efficient emitters will be required in order to fabricate mid-IR QD lasers. The two fundamental parameters which must be improved are the scattering/tunneling lifetimes of electrons in the excited and ground states of the dots, respectively. For electrons in the excited states, electrons must be prevented from escaping before they are able to make an optical transition to the dot ground state, while electrons in the dot ground state must be extracted efficiently into either an electron energy filter or the continuum.

A novel method for improving both of the above parameters utilizes the three-dimensional geometry of the quantum dots themselves (Figure 6). Models of quantum dots have determined that the electron ground state wavefunction is s-type, positioned in the center of the dot, while the first excited states are p-type in nature and sit towards the edges of the dot [9]. If the quantum dot is capped by a thin AlGaAs layer, electrons in the center of the dot see a thin AlGaAs barrier to the continuum, allowing efficient extraction from the dot for electrons in the lower states. Electrons positioned towards the edges of the dot, however, will see a significantly thicker AlGaAs barrier to the continuum, preventing escape from the excited states of the dot. By controlling the AlGaAs cap layer thickness, one can effectively exercise control over

SPIE USE: ____ DB Check, ____ Prod Check, Notes:

Please verify that (1) all pages are present, (2) all figures are acceptable, (3) all fonts and special characters are correct, and (4) all text and figures fit within the margin lines shown on this review document. Return to your MySPIE ToDo list and approve or disapprove this submission.

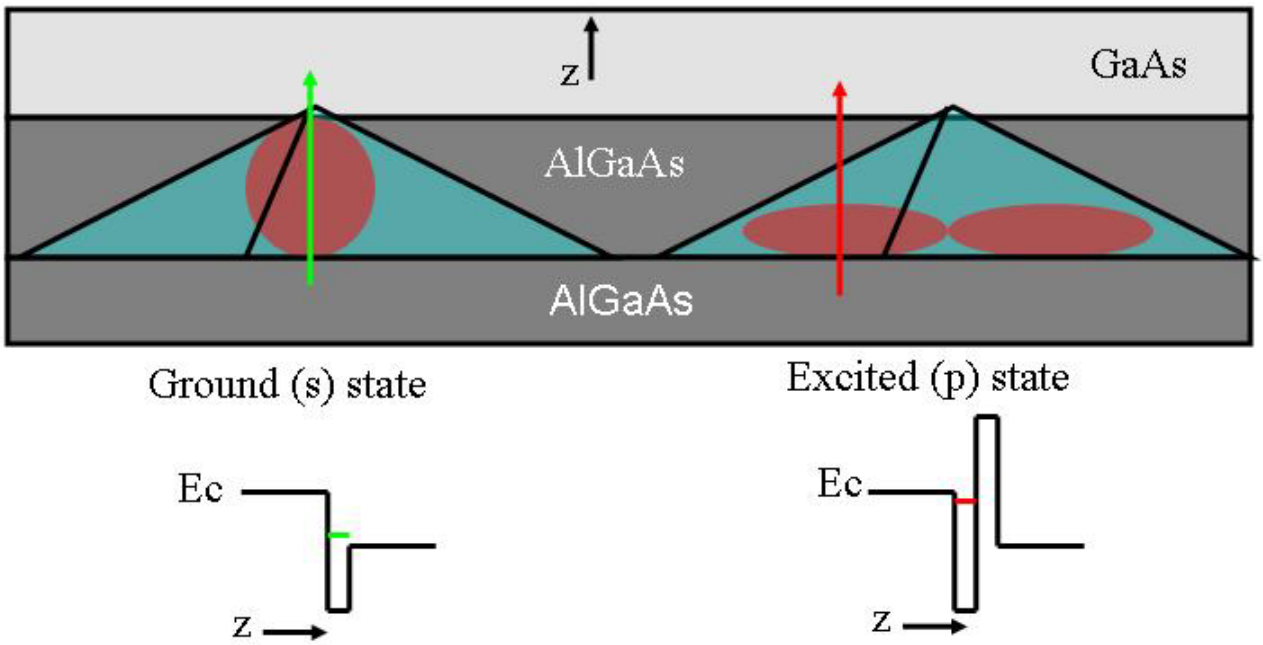

Fig. 6. chematic of growth structure for improved QD mid-IR emitter. The QDs, in this schematic, are modeled as pyramids, and the approximate energy states are shown in red. The dots are grown on an AlGaAs injector, and covered by an AlGaAs cap layer, followed by GaAs. Below the growth structure are two conduction band profiles. The first shows the conduction band for an electron in the quantum dot ground state (note the weak confinement of the state on the downstream side of the dot), while the second shows the conduction band structure for an electron in an excited dot state (here there exists a barrier for exit from the dot which serves to lengthen the escape time from the quantum dot excited state)

electron lifetimes in the excited and ground states of the quantum dot. At the same time, a graded AlGaAs injector allows for high energy injection into QD excited states, while the Al content of the cap layer and injector can effectively control the position of the QD electron ground state with respect to the GaAs bandedge, allowing the design of structures with QD ground states above the GaAs bandedge, an additional advantage for decreasing extraction times from the QD ground state. Such samples are currently under investigation, and studies are underway to determine the necessary Al content of the injector and cap layers required to position the QD ground state energy above the GaAs bandedge.

4. CONCLUSIONS

Mid-IR electroluminescence from InAs self-assembled quantum dots in unipolar cascade-like structures has been demonstrated. While initial emission intensities were weak, they showed a clear quantum dot emission signal distinct from any possible heating effects. Improved design of the device injector and extractor regions show a marked improvement in emission intensity, suggesting that further improvements in device design will allow for even stronger emission. Additionally, multiple wavelength emission has also been seen from select samples, and this emission shows a distinct polarization in the growth plane. A qualitative analysis of this data suggests that the polarization seen from these samples can be attributed to an anisotropic growth morphology of InAs QDs on AlAs surfaces. This assertion is supported by previous independent studies on anisotropic photoconductivity and in-situ growth morphology of QDs on AlAs. Our work, however, is the first example of growth morphology studies performed by means of electroluminescence spectroscopy measurements. We have also presented both proposed and realized methods for improving emission from our devices. Studies of contact geometries for our emitters suggest that an improved emission efficiency can be achieved by more efficient electrical contacting of our dot layer. Additional improvements in device

SPIE USE: ____ DB Check, ____ Prod Check, Notes:

Please verify that (1) all pages are present, (2) all figures are acceptable, (3) all fonts and special characters are correct, and (4) all text and figures fit within the margin lines shown on this review document. Return to your MySPIE ToDo list and approve or disapprove this submission.

efficiency may be achieved by utilizing the geometry of the quantum dots themselves in order to control both the lifetimes of electron dot states and the energy position, relative to the GaAs bandedge, of states in the dots.

The utilization of InAs quantum dots to provide three-dimensional confinement in quantum cascade structures for mid-IR emission is a promising route to both increased efficiency in mid-IR emitters and vertically emitting mid-IR laser devices. While initial results utilizing quantum dots showed weak emission, significant improvements in both emission intensity and efficiency have been shown by optimizing sample design and device fabrication. Additionally, multiple wavelength emission from these devices suggests a broader spectral range for QD mid-IR emitters than initially thought possible. These advances, and improvements to device design currently under investigation, suggest the possibility of developing a novel class of mid-IR emitting devices.

REFERENCES

1. J. Faist, F. Capasso, D.L. Sivco, C. Sirtori, A.L. Hutchinson, and A.Y. Cho, Quantum Cascade Laser, *Science*, 264, 553-556 (1994).
2. J.S. Yu, S. Slivken, S.R. Darvish, A. Evans, B. Golden, and M. Razeghi, "High-power, room-temperature, and continuous-wave operation of distributed-feedback quantum-cascade lasers at λ~4.8μm", *Appl. Phys. Lett.*, 87, 041104-6 (2005).
3. C. Gmachl, D.L. Sivco, R. Colombelli, F. Capasso, and A.Y. Cho, "Ultra-broadband semiconductor laser", *Nature*, 415, 883-887 (2002)
4. C-F. Hsu, J.S. O, P. Zory, and D. Botez, "Intersubband laser design using a quantum box array", *Proc. SPIE 3001*, 271 (1997).
5. D. Smirnov, C. Becker, O. Drachenko, V.V. Rylkov, H. Page, J. Leotin, and C. Sirtori, "Control of electron-optical scattering rates in quantum box cascade lasers", *Phys. Rev. B*, 66, 121305 (2002).
6. R. Colombelli, K. Srinivasan, M. Troccoli, O. Painter, C. Gmachl, D.M. Tennant, A.M. Sergent, D.L. Sivco, A.Y. Cho, and F. Capasso, "Quantum Cascade Surface-Emitting Photonic Crystal Laser", *Science*, 1374-1377 (2003).
7. C. Pflügl, M. Austerer, W. Schrenk, S. Golka, G. Strasser, R.P. Green, L.R. Wilson, J.W. Cockburn, A.B. Jrysa and J.S. Roberts, "Single-mode surface-emitting quantum-cascade lasers", *Appl. Phys. Lett.*, 86, 211102 (2005).
8. P. Ballet, J.B. Smathers, and G.J. Salamo, "Morphology of InAs self-organized islands on AlAs surfaces", *Appl. Phys. Lett*., 75, 337 (1999).
9. E. Finkman, S. Maimon, V. Immer, G. Bahir, S.E. Schacham, F. Fossard, F.H. Julien, J. Brault, and M. Gendry, "Polarized front-illumination response in intraband quantum dot infrared photodetectors at 77 K", *Phys. Rev. B*, 63, 045323 (2001).
10. O. Stier, M. Grundmann, and D. Bimberg, "Electronic and optical properties of strained quantum dots modeled by 8-band kp theory", *Phys. Rev. B*, 59, 5688-5701 (1999).

SPIE USE: ____ DB Check, ____ Prod Check, Notes: